Cellular Physiology and Biochemistry

Cell Physiol Biochem 2018;48:741-752
DOI: 10.1159/000491903
Published online: July 19, 2018
Accepted: June 05, 2018

Original Paper

Identification of the C-Reactive Protein Interaction Network Using a Bioinformatics Approach Provides Insights into the Molecular Pathogenesis of Hepatocellular Carcinoma

Sha She Lingyu Jiang Zhenfang Zhang Min Yang Huaidong Hu Peng Hu Yong Liao Yixuan Yang Hong Ren

Institute for Viral Hepatitis, Key Laboratory of Molecular Biology for Infectious Diseases (Ministry of Education), Department of Infectious Diseases, The Second Affiliated Hospital, Chongqing Medical University, Chongqing, China

Key Words
C-reactive protein (CRP) • Isobaric Tags for Relative and Absolute Quantitation (iTRAQ) • Gene Ontology (GO) • Kyoto Encyclopedia of Genes and Genomes (KEGG)

Abstract
Background/Aims: C reactive protein (CRP) levels are elevated in many diseases, including malignant tumors and cardiovascular disorders. In this study, the protein interaction network for CRP was evaluated to determine the importance of CRP and its interacting proteins in the molecular pathogenesis of hepatocellular carcinoma (HCC). ***Methods:*** Isobaric tags for relative and absolute quantitation (iTRAQ) and mass spectrometry were used to identify CRP interacting proteins in SMMC7721 cells. Moreover, Gene Ontology (GO) and the Kyoto Encyclopedia of Genes and Genomes (KEGG) were used to evaluate enriched genes and pathways for differentially expressed genes using DAVID and WebGestalt. Co-immunoprecipitation and western blot analyses were employed to assess interactions between CRP and KRT8, ANXA2, ENO2, and HSP90B1. ***Results:*** In total, 52 proteins that interact with CRP were identified. A GO analysis suggested that most of the interacting proteins were involved in CRP complexes and regulated metabolic processes. A KEGG pathway analysis suggested that most CRP-interacting proteins contribute to the TRAIL signaling pathway, Class I PI3K/Akt signaling pathway, plasma membrane estrogen receptor signaling, Nectin adhesion pathway, and S1P1 pathway. Immunoprecipitation and western blot analyses revealed interactions between CRP and KRT8, ANXA2, ENO2, and HSP90B1. ***Conclusions***: iTRAQ based proteomic profiling revealed the network of CRP interacting proteins. This network may activate the PI3K/Akt signaling pathway, thereby contributing to the pathogenesis of HCC.

S. She, L. Jiang and Z. Zhang contributed equally to this work.

Prof. Yixuan Yang
and Hong Ren

Department of Infectious Diseases, The Second Affiliated Hospital of Chongqing Medical University 76# Linjiang Road, Chongqing 400010 (China)
Tel. 86 23 63693215, Fax 86 23 63693215, E-Mail yummy_8813@sina.com

Introduction

Hepatocellular carcinoma (HCC) is the most common primary malignant cancer affecting the liver. It is the fifth and seventh most common type of cancer affecting men and women, respectively, and is categorized as the second most common cause of cancer deaths among men and sixth most common cause of cancer deaths among women [1-3]. HCC has several known risk factors, including chronic hepatitis B virus and hepatitis C virus infections, liver cirrhosis, and several metabolic diseases [4-6]. Liver injury induced by these risk factors produces a progressive inflammatory milieu that results in a cycle of necrosis and regeneration and the development of chromosomal instability [7]. Genetic, proteomic, and epigenetic alterations that progressively accumulate in a background of increased reactive oxygen species, inflammatory cytokines, and fibrosis likely lead to the initiation of HCC [8]. The initiation and progression of HCC occur by multiple steps, but the precise molecular events that underlie HCC formation remain only partially understood.

Since the quantitative potential of proteomics was initially demonstrated, efforts have been made to develop and improve quantitative methods (e.g., ICAT[9], iTRAQ [10, 11], SILAC [12, 13], and label free methods [14]). These endeavors have focused primarily on obtaining high throughput quantitative information about the abundance of proteins at the scale of biological systems [6, 15, 16]. Since biological activity is executed directly by proteins, proteomic analyses of diseases or stages of diseases may shed light on the etiopathogenesis and deepen our understanding of these diseases, and may provide a basis for the development of improved treatment strategies. The iTRAQ method is considered a particularly powerful tool, since it can facilitate the simultaneous analysis of up to eight samples in a single experiment. Several features of iTRAQ, such as its high through-put ability, wide range of separation, high accuracy, and repeatability, have led to its widespread use in proteomics.

C reactive protein (CRP), the first acute phase protein described, is an ancient and highly conserved member of the pentraxin family; it has five identical subunits forming a planar ring that confers very high stability to the protein [17]. It is mainly synthesized by hepatocytes in response to various inflammatory stimuli [18]. The risk of cancer is increased when pre-diagnostic CRP levels are high [19]. Our previous results suggest a close relationship between CRP and HCC, and CRP levels are highly correlated with the extent of liver cancer invasion and migration [20]. Despite extensive clinical evidence for a role of CRP in the pathogenesis of HCC, an underlying molecular mechanism has not yet been identified.

With the development of proteomics, increasing studies have indicated that molecular functions and biological processes in cells are coordinated by protein complexes or protein networks, and protein–protein interactions have been a focus of cancer research. Co-immunoprecipitation (Co-IP) combined with mass spectrometry (MS) has become the method of choice for identifying protein–protein interactions [21, 22]. The identification of interacting proteins is an important way to understand the functions of CRP. Based on our previous study, we screened CRP interacting proteins a using a targeted proteomics approach (Co-IP coupled with iTRAQ based MS) to clarify the CRP related network and its role in the molecular pathogenesis of HCC.

Materials and Methods

Reagents and antibodies

Eight plex iTRAQ Reagent Kits were acquired from Applied Biosystems (Foster City, CA). Monoclonal antibodies against human CRP were obtained from HyTest (Finland, Turku), and the anti-Cytokeratin 8, anti-Annexin A2, anti-ENO2, and anti-HSP90B1 antibodies were purchased from Abcam (Cambridge, MA). CRP-specific Stealth Select RNAi™ small interfering RNA (siRNA) (NM_000567), Stealth RNAi™ Negative Control siRNA, and Lipofectamine Max transfection reagent were obtained from Santa Cruz Biotechnology (Santa Cruz, CA). Small interfering RNAs against human ENO2 (ID121346, ID 121348) and HSP90B1 (ID119655, ID

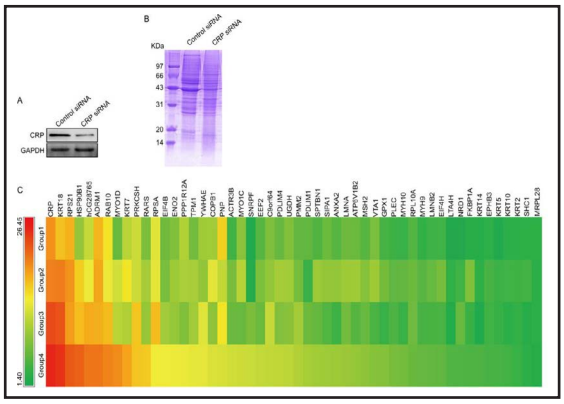

Fig. 1. Inhibition efficiency of CRP siRNA and heat map of CRP interacting proteins. (A). SMMC7721 cells were transfected with CRP-targeted siRNAs. Effective silencing of CRP was tested by western blotting. (B) The differential strip of the control and siCRP group evaluated by MS. (C). The color scale shown at the top illustrates the fold change in protein expression for each group. 118:113 and 121:119 refer to relative levels of protein expression in SMMC7721 cells transfected with control siRNA with respect to cells transfected with CRP siRNA (group 1 and group 2, 118:113; group 3 and group 4, 121:119; group 1 and group 3 were biological duplicates; group 2 and group 4 were technical duplicates). Statistical analyses for iTRAQ-based detection and relative quantification were implemented using the Paragon Algorithm in ProteinPilot.

119656) were purchased from Invitrogen (Grand Island, NY). IP lysis buffer was purchased from Beyotime (Shanghai, China). Protein A/G agarose beads were obtained from GE Healthcare (Little Chalfont, UK).

Cell culture

Human liver cell lines SMMC7721 and Huh7 were cultured in high glucose DMEM containing 10% fetal bovine serum and 1% penicillin-streptomycin solution. They were maintained at 37°C in a humidified chamber with an atmosphere of 5% CO_2 until use.

CRP siRNA transfection, co-immunoprecipitation, and iTRAQ labeling

SMMC7721 cells were transfected with 100 nM CRP-specific siRNA or a negative siRNA using Lipofectamine Max. CRP-specific siRNA effectively silenced CRP expression (Fig. 1A). SMMC7721 cells were then trypsinized and lysed in 1 ml of lysis buffer on ice for 20 min after 48 h. Cell lysates were centrifuged for 30 min at 13, 000 rpm and 4°C. One milligram of the lysate (1 μg/μl) was mixed with 2 μg of CRP antibodies overnight at 4°C. Protein G beads were added to the immune complexes and incubated for 2 h under gentle agitation at 4°C. The beads were pelleted and washed three times with lysis buffer. Bound proteins were eluted in sodium dodecyl sulfate (SDS) sample buffer, subjected to SDS-polyacrylamide gel electrophoresis (PAGE), and analyzed by immunoblotting. The eluted protein (300 μg) was precipitated from each pooled group, dissolved in dissolution buffer, denatured, cysteine blocked, digested with 2 μg of sequencing grade modified trypsin, and labeled using iTRAQ reagents (Control siRNA, 118 and 121 tag; CRP siRNA 113 and 119 tag) provided with the iTRAQ Kit. Peptides from each sample set were mixed prior to subsequent analyses.

Mass spectrometry

Labeled peptides were fractionated and purified by immobilized-pH-gradient isoelectric focusing, as previously described [23, 24]. Purified peptide fractions were reconstituted in solvent A (water/ACN [98:2 v/v] with 0.1% formic acid) and separated using a C18-PepMap column (Thermo Fisher Scientific, Beijing, China) with a solvent gradient of 2–100% Buffer B (0.1% formic acid and 98% acetonitrile) in Buffer A at a flow rate of 0.3 μl/min. The peptides were electrosprayed using a nanoelectrospray ionization source at an ion spray voltage of 2300 eV and analyzed by a NanoLC-ESI-Triple TOF 5600 system (AB Sciex, Framingham, MA). The mass spectrometer was set to positive ion mode at a mass range of 300–1800 m/z. The two most intensely charged peptides above 20 counts were selected for MS/MS at a dynamic exclusion of 30 s [25]. Data were processed using ProteinPilot v2.0 (AB Sciex) and compared with the International Protein Index Human database v3.77. Cysteine modified by methane thiosulfate was specified as a fixed modification. Protein identification was based on a threshold protein score of >1.3. For quantitation, at least two unique peptides with 95% confidence and a P-value less than 0.05 were required.

Bioinformatic analysis

The differentially expressed proteins and differently expressed genes (DEGs) between the control siRNA group and CRP siRNA group were identified using ProteinPilot™. For protein identification, a confidence limit of 95% and a false discovery rate of 5% were used, and an additional threshold of less than 1.3 was applied to all iTRAQ ratios to minimize false positives for the determination of upregulated proteins. The significant gene ontology (GO) biological process terms and Kyoto Encyclopedia of Genes and Genomes (KEGG) pathways for the identified DEGs were evaluated using the Database for Annotation, Visualization, and Integrated Discovery (DAVID) and the WEB-based GEne SeT AnaLysis Toolkit (WebGestalt).

Western blotting

Western blot analyses were performed to validate the proteomic results using randomly chosen CRP-interacting proteins. SMMC7721 and Huh7 cell protein samples were collected in lysis buffer. Then, 1 mg of lysate (1 μg/μl) was mixed with 2 μg of CRP antibodies overnight at 4°C and 20 μl of Protein G beads for 2 h under gentle agitation at 4°C, and bound proteins were eluted in an equal volume of SDS sample buffer. Equal volumes of diluted samples were separated by SDS-PAGE and transferred onto polyvinylidene fluoride membranes. Membranes were blocked in 5% skim milk in Tris-buffered saline with Tween20, and incubated with primary antibodies against KRT8, ANXA2, ENO2, and HSP90B1. The membranes were then incubated with the horseradish peroxidase conjugated secondary antibody at room temperature. Finally, membranes were visualized using an electrochemiluminescence detection instrument (Bio-Rad Laboratories, Hercules, CA).

Table 1. The list of Proteins Found to Be Expressed at Different Levels between Control siRNA group and CRP siRNA group by iTRAQ Analysis

Accession	Gene sym	Coverage	Peptides	Fold change	*p* Value
Q13084	MRPL28	24.609999	2	2.506169081	0.0032652
Q03252	LMNB2	31.61	6	6.168507099	0.0056332
Q15149	PLEC	37.380001	27	7.597248554	0.0004678
Q9P1U1	ACTR3B	19.62	2	13.11625004	0.0016779
P29353	SHC1	21.610001	2	3.123962879	0.0272561
P62942	FKBP1A	36.55	4	4.961688995	0.0130626
P02545	LMNA	48.640001	21	9.890003204	0.0010584
O14974	PPP1R12A	23.59	6	14.82450199	3.68E-05
P54753	EPHB3	21.04	2	4.668119431	0.0048548
P02533	KRT14	50.639999	24	4.90069294	0.0005633
P21281	ATP6V1B2	23.48	2	9.66032505	0.0161578
Q15056	EIF4H	60.479999	7	6.00445509	0.0230626
P35579	MYH9	25.870001	18	6.234810829	0.0004855
P13639	EEF2	18.529999	7	12.41300201	0.0146423
P35580	MYH10	23.84	6	7.202699661	0.0336321
O43847	NRD1	16.74	2	5.010097027	0.0023063
P62906	RPL10A	17.97	2	6.514740944	0.0048548
P09493	TPM1	51.999998	19	14.5096817	0.012117
O94832	MYO1D	23.16	2	20.67488098	0.0050952
Q5T6V5	C9orf64	21.41	2	12.35050011	0.0198286
P02741	CRP	21.55	3	26.44661903	7.294E-05
P23588	EIF4B	43.020001	6	15.20006847	0.0052671
P63220	RPS21	53.009999	3	23.45479202	0.007298
P08865	RPSA	31.439999	3	15.32111645	0.0005267
P09104	ENO2	21.2	4	15.04630566	0.0001212
P61026	RAB10	27.500001	2	21.20749283	0.0005095
P54136	RARS	27.419999	4	17.34619141	0.0016973
P43246	MSH2	23.450001	2	9.085041046	0.0261578
P09960	LTA4H	14.89	2	5.184479237	0.0013063
O15305	PMM2	37.580001	5	11.19757175	0.0174821
O00151	PDLIM1	24.62	2	10.67100239	0.0003415
O60701	UGDH	27.73	3	11.98338509	0.0298286
Q01082	SPTBN1	26.120001	11	10.28498173	0.0017482
P13645	KRT10	61.129999	36	4.457110882	2.34E-07
P62258	YWHAE	32.94	5	14.35660934	0.0002139
P50479	PDLIM4	34.549999	2	12.2376852	0.0194912
P35908	KRT2	60.56	34	3.858566761	0.0082652
P13647	KRT5	46.270001	36	4.572263241	2.34E-07
P53618	COPB1	17.209999	2	13.80867481	0.0148917
P14314	PRKCSH	16.069999	2	17.61119461	0.0213924
P14625	HSP90B1	37.130001	7	23.05605888	0.0007294
P00491	PNP	38.010001	2	13.5888443	0.0037482
Q96FS4	SIPA1	37.810001	7	10.18189049	0.0034148
P05787	KRT8	48.449999	26	25.69271469	0.0028967
O00159	MYO1C	31.510001	9	12.95617867	0.0004678
P62306	SNRPF	29.069999	3	12.83819485	0.0014642
P07355	ANXA2	35.100001	8	10.0636816	1.50E-05
P08729	KRT7	61.830002	26	19.39723015	0.0101146
Q9NP79	VTA1	25.709999	2	8.549180031	0.0052671
P07203	GPX1	27.720001	2	8.420338631	0.0046781
Q16186	ADRM1	16.71	3	21.94843292	0.0289668
A0A024R152	hCG28765	14.36	3	22.01866913	0.0021392

Confocal Microscopy

SMMC7721 and Huh7 cells at a density of 1×10^5 cells per confocal culture dish were cultured with DMEM supplemented with 10% fetal bovine serum for 24 h. Then, cells were fixed with 10% (vol/vol) paraformaldehyde, perforated with 0.1% (vol/vol) Triton X-100, and blocked with 10% (vol/vol) normal goat serum in phosphate-buffered saline with Tween-20. Cells were incubated for 18 h in anti-CRP, anti-ENO2, and anti-HSP90B1 primary antibodies and were subsequently incubated in the appropriate species-specific Alexa fluorescent dye-conjugated secondary antibodies (Invitrogen) for 90 min at 37°C. The immunostained cells were viewed by confocal microscopy (Nikon, Melville, NY).

ENO2 and HSP90B1 siRNA transfection

ENO2 or HSP90B1 siRNA was used for transfection into SMMC7721 and Huh7 cells according to protocols provided by Invitrogen. CRP expression was monitored by western blotting.

Results

iTRAQ quantification of the CRP interactome

To investigate CRP interacting proteins, a targeted and quantitative proteomics analysis using Co-IP coupled with iTRAQ based MS was performed. Two or more peptides were used for quantification and protein identification. Differential expression between the control and siCRP group based on MS is summarized in Fig. 1B. For Protein Pilot based database searching and identification, the threshold [unused protscore (conf)] was set to 95% confidence at a 5% FDR. Additionally, a ProtScore value of greater than 1.3 was used to attain a confidence of 95%. When proteins were classified as significantly differentially regulated or not, an additional 1.3 (1 × 1.3)-fold cutoff was applied to all iTRAQ ratios to minimize false positives when identifying proteins as upregulated. This cutoff value is widely employed in iTRAQ analyses [20]. In total, 52 unique proteins were successfully identified (fold change > 1.3 and $p < 0.05$) in the control siRNA group compared with the CRP siRNA group (Table 1). A hierarchical clustering heat map of the differentially expressed proteins is shown in Fig. 1C.

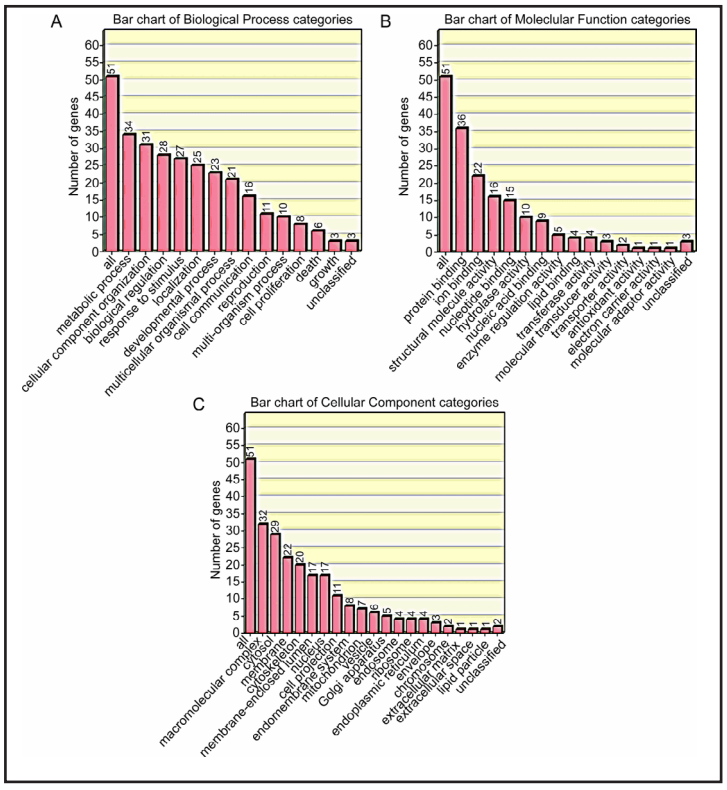

Fig. 2. GO term enrichment analysis of CRP-interacting proteins. Proteins identified by iTRAQ categorized by (A) biological process, (B) molecular function, and (C) cellular component using the WebGestalt (WEB-based gene set analysis toolkit) Classification System (http://www.webgestalt.org/option.php).

GO term enrichment analysis of CRP interacting proteins

The results of the GO term enrichment analysis varied depending on GO classification and expression changes of DEGs. In total, 52 DEGs were uploaded to the online software DAVID and WebGestalt to identify overrepresented GO categories for an enrichment analysis. As shown in Fig. 2, the enriched biological process terms (BP, Fig 2A) were primarily metabolic process (34, 66.7%), cellular component organization (31, 60.7%), biological regulation (28, 54.9%), response to stimulus (27, 52.9%), and localization (25, 49.0%). The enriched molecular function terms (MF, Fig 2B) were mainly protein binding (36, 70.5%), ion binding (22, 43.1%), structural molecule activity (16, 31.3%), nucleotide binding (15, 29.4%), and hydrolase activity (10, 19.6%). In an analysis of cellular components (CC, Fig 2C), proteins were primarily enriched for the terms macromolecular complex (32, 62.7%), cytosol (29, 56.8%), membrane (22, 43.1%), cytoskeleton (20, 39.2%), and membrane-enclosed lumen (17, 33.3%).

KEGG pathway enrichment analysis

Using the KEGG pathway database, the CRP interactome was classified into 65 pathways, the top 20 of which are shown in Fig. 3. The TRAIL signaling pathway was the top

pathway, followed by the Class I PI3K/Akt signaling pathway, plasma membrane estrogen receptor signaling, Nectin adhesion pathway, and S1P1 pathway. The KEGG maps related to the Class I PI3K/Akt signaling pathway suggest a fairly complicated molecular mechanism underlying HCC, as shown in Fig. 4.

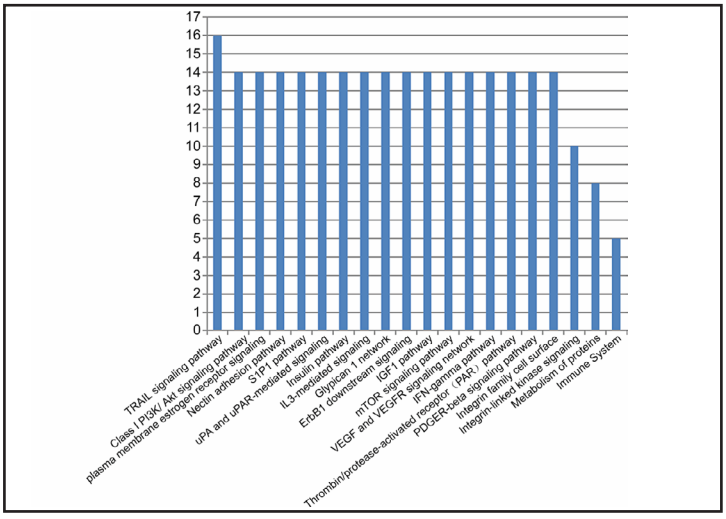

Fig. 3. KEGG pathway enrichment analysis. KEGG pathway analysis of identified proteins. Vertical bars represent the number of identified proteins.

Disease enrichment analysis of the CRP interactome

Based on a disease enrichment analysis, CRP and CRP interacting proteins were primarily involved in skin diseases, cardiovascular diseases, metabolic diseases, and carcinoma (data not shown). Fig. 5 shows several diseases in liver, metabolic diseases, neoplasms, and syndromes associated with these proteins.

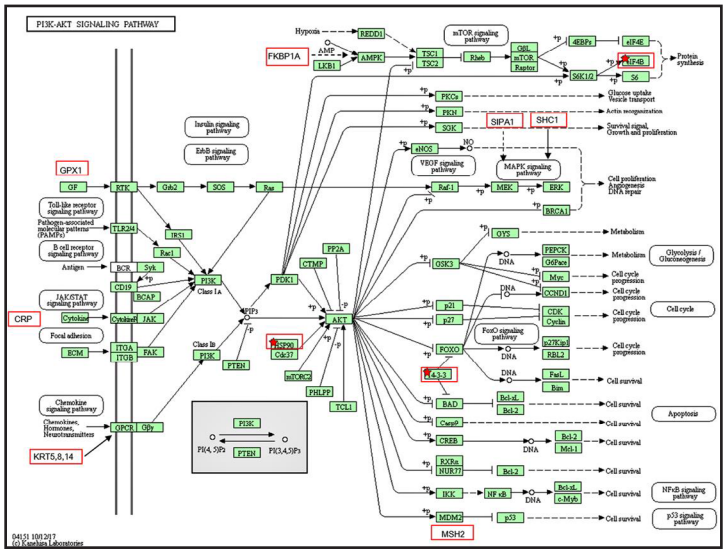

Fig. 4. Class I PI3K/Akt signaling pathway map. KEGG pathway enrichment analysis the map of the Class I PI3K/Akt signaling pathway. Proteins in red frames are differentially expressed proteins identified in this study. The solid arrow indicates activation; the dashed arrow indicates indirect activation.

Protein verification by western blotting and immunofluorescence

Our proteomics analysis revealed many interesting protein interactions for CRP. To determine the reliability of the iTRAQ results, we selected several protein candidates and confirmed their expression by Co-IP and western blotting. As expected, KRT8, ANXA2, ENO2, and HSP90B1 were captured when CRP was used as the bait protein (Fig. 6 A). To further explore *in vivo* interactions, subcellular localization studies were performed. Confocal microscopy of cells co-labeled with antibodies recognizing CRP and ENO2 or HSP90B1 revealed co-localization within the HCC cells SMMC7721 and Huh7 (Fig 6B). The percentage of CRP co-localizing with either ENO2 or HSP90B1 was analyzed and quantified using ImageJ (co-localization was identified by yellow areas, and scatter plots and Pearson correlation coefficients indicated the relationship between CRP and ENO2 or HSP90B1).

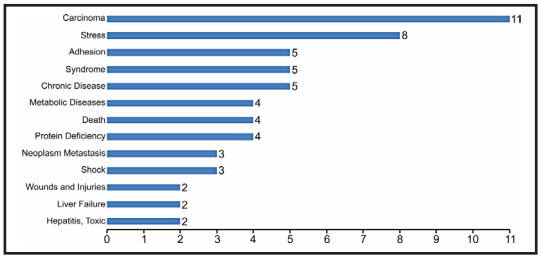

Fig. 5. Disease enrichment analysis of the CRP interactome. Disease enrichment analysis of identified proteins by co-immunoprecipitation coupled with iTRAQ based MS. The vertical bars represent the number of identified proteins.

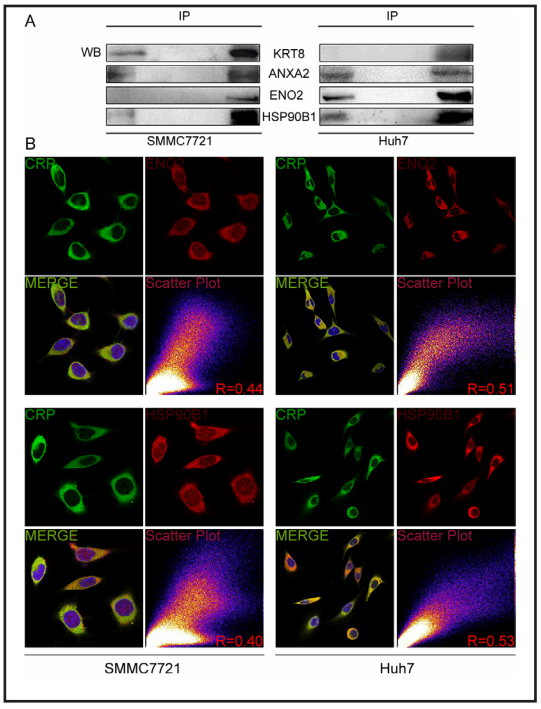

Fig. 6. Confirmation of interactions between CRP and proteins identified by the MS analysis in the hepatoma cell lines SMMC7721 and Huh7. (A). Co-immunoprecipitation was employed to validate the protein–protein interactions predicted by iTRAQ-mass spectrometry. CRP-specific antibodies were used to capture CRP-binding proteins. Co-immunoprecipitation with normal rabbit IgG or not served as a negative control. Interactions between CRP and KRT8, ANXA2, ENO2, or HSP90B1 were successfully validated. (B) Co-localization of CRP with proteins identified by MS using immunofluorescence. Hepatoma cells SMMC7721 and Huh7 were stained with an anti-CRP antibody and an anti-ENO2 or anti-HSP90B1 antibody, followed by incubation with FITC-conjugated donkey anti-rat IgG (for ENO2, HSP90B1) or PE-conjugated goat anti-mouse IgG (for CRP) and visualization using a confocal microscope. (Co-localization was identified by the yellow areas, and scatter plots and Pearson correlation coefficients indicated the relationship between CRP and ENO2 or HSP90B1).

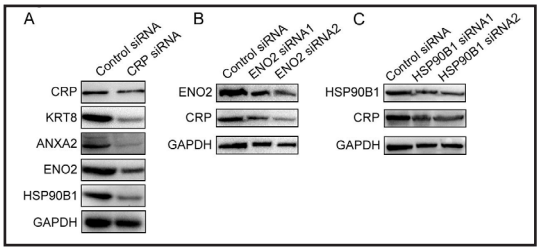

Fig. 7. Western blot analysis of KRT8, ANXA2, ENO2, and HSP90B1. (A) Protein levels in HCC cells transfected with CRP-specific or control siRNAs were analyzed by western blotting. The protein expression of CRP in SMMC7721 cells transfected with ENO2-specific siRNA (B) or HSP90B1-specific siRNA (C).

Knockdown of ENO2 or HSP90B1 suppresses CRP protein expression

High levels of CRP may play a role in cancer invasion, metastasis, and poor prognosis, and some CRP interacting proteins are involved in these processes. Experimental results indicated that CRP interacts with KRT8, ANXA2, ENO2, or HSP90B1 *in vivo* or *in vitro*. We examined the role of CRP in HCC development via interactions with KRT8, ANXA2, ENO2, or HSP90B1. SiRNA was used to knock down CRP in HCC cells, and the expression levels of KRT8, ANXA2, ENO2, and HSP90B1 were evaluated. As shown in Fig. 7A, the levels of KRT8, ANXA2, ENO2, and HSP90B1 decreased in response to CRP knock down, suggesting that CRP modulates the expression of these proteins. Furthermore, the expression of CRP also decreased in response to the knock down of ENO2 or HSP90B1 in HCC cells (Fig. 7B, C). These results indicated that ENO2 or HSP90B1 may stimulate the secretion of CRP, thereby promoting the progression of HCC.

Discussion

CRP is secreted in response to pro-inflammatory stimuli and acts in an autocrine/paracrine fashion [26-29]. CRP levels are elevated in patients with infections, inflammatory diseases, necrosis, myocardial infarction [30], and malignancies, including multiple myeloma [31, 32], lymphoma [33, 34], and carcinoma [35, 36]. CRP binds to various ligands, including pneumococcal polysaccharides, membrane phospholipids, apoptotic cells, fibronectin, and ribonuclear particles [17, 37]. Therefore, it is important to obtain the CRP interacting protein network to clarify the molecular pathogenesis of diseases.

CRP is a diagnostic and prognostic marker in a diverse range of cancers, from localized to systemic cancer [38, 39]. We previously detected a close relationship between CRP and HCC. To elucidate the molecular mechanism underlying the role of CRP in HCC, we identified the CRP interacting protein network in the hepatoma cell line SMMC7721 by Co-IP, iTRAQ, and MS. We adopted very stringent criteria to filter out proteins that were identified in two independent biological replications and two experimental replications. We identified 52 proteins that interact with CRP (Table 1). Then, we performed a bioinformatics analysis of the identified proteins using DAVID and the WebGestalt toolkit.

According to GO annotation and enrichment analyses, the interacting proteins in hepatoma cells were primarily involved in macromolecular complexes and were located in the cytosol and membrane. Based on its sequence and binding specificity, CRP may contribute to the pathogenesis of HCC by binding to these receptor complexes. With respect to MF, CRP-interacting proteins were mainly involved in protein binding, structural molecule activity, and cell–cell adhesion. With respect to the BP category, CRP and its interactome participated in the regulation of metabolic processes, cell–cell adhesion, viral processes, and angiogenesis. These results suggest that CRP can regulate different biological processes in tumor cells via interactions with these key proteins, including KRT8, ANXA2, ENO2, and HSP90B1.

According to a KEGG pathway enrichment analysis, the TRAIL signaling pathway, Class I PI3K/Akt signaling pathway, plasma membrane estrogen receptor signaling, Nectin adhesion pathway, and S1P1 pathway were the top five significantly enriched pathways. Most identified CRP interacting proteins were enriched for these pathways. We evaluated a signaling pathway of interest, namely, the PI3K/ Akt signaling pathway, as shown in Fig. 4. We found that CRP and CRP interacting proteins have different roles in the PI3K/Akt signaling pathway. CRP acts as a cytokine, binds to cytokine receptors (ANXA2, KRT8, and EPHB3), activates PI3K, regulates protein or protein kinases, stimulates the expression of phosphorylated Akt, phosphorylated MAPK, phosphorylated ERK, metabolic process related proteins, or biological process related proteins within cells (HSP90B1, EIF4B, SIPA1, SHC1, and MSH2), and regulates cell growth, proliferation, survival, apoptosis, and metabolism. Carcinogenesis is the result of a disruption of the balance between cell division and growth on the one hand and programmed cell death on the other [40]. In the context of this delicate balance, proteins and signaling pathways that regulate cell growth, differentiation, and development undergo oncogenic changes far more often than do other groups of molecules. It has recently been shown that the TRAIL signaling pathway, PI3K/Akt signaling pathways, Nectin adhesion pathway, and S1P1 pathway, which are involved in these and other processes, are frequently disturbed in many human cancers [40-43]. HCC is a highly prevalent, treatment resistant malignancy with a multifaceted molecular pathogenesis. The underlying mechanisms have been linked to alterations in several important cellular signaling pathways. These pathways are of interest from a therapeutic perspective; they are potential targets to reverse, delay, or prevent tumorigenesis. An early study showed that the PI3K/AKT/mTOR signaling pathway can be overactivated by the enhanced stimulation of receptor tyrosine kinases, particularly the IGF receptor and EGFR. Both IGF and IGF receptor are upregulated in HCC and human cirrhotic livers, resulting in the stimulation of the PI3K/AKT/ mTOR signaling pathway [44]. Thus, the CRP interactome may participate in various signaling pathways (including the vascular endothelial growth factor [VEGF] and VEGF receptor signaling network, PDGFR-

beta signaling pathway, and IFN-gamma pathway) and in the immune system, thereby regulating HCC carcinogenesis.

Based on a disease enrichment analysis, CRP and CRP-interacting proteins were primarily involved in skin diseases, cardiovascular diseases, metabolic diseases, and carcinoma (data not shown). Fig. 5 shows several diseases in liver, metabolic diseases, neoplasms, and syndromes related to these proteins. These results indicated that some key proteins may directly regulate diseases. High levels of these proteins in circulation are closely related to the occurrence, progression, and prognosis of diseases.

Based on the results of the GO and KEGG analyses, we selected four key protein candidates that mediate tumor progression or play an important role in related signaling pathways. We discuss these key proteins in the following text.

ENO2 (Gamma-enolase) is an intracellular enzyme that catalyzes the dehydration of 2-phospho-D-glycerate to phosphoenolpyruvate in the catabolic direction of the glycolytic pathway. The glycolytic pathway and its enzymes are among the most highly conserved and important metabolic networks and have pleiotropic effects in physiological and pathological processes, including cancer. For instance, ENO2 may bind to actin and tubulin, mediate invasiveness and microtubule motility in tumor cells, and increase the phosphoprotein levels of the PI3K/Akt signaling pathways [45]. HSP90B1 is an endoplasmic reticulum protein; it chaperones and aids in the folding of client proteins, including Toll-like receptors, Wnt coreceptor LRP6, insulin-like growth factors, and integrin [46]. Hepatocytes are highly metabolic cells with active protein synthesis and secretory machinery, including coagulation factors, complement proteins, C reactive protein, and many others involved in ER maintenance and efficient stress responses. A previous study suggested that gp96 is an oncogenic chaperone in hepatocyte carcinogenesis and a promising therapeutic target for liver cancer [46]. We found that ENO2 and HSP90B1 were significantly down-regulated when CRP was silenced, indicating that the depletion of CRP inhibited ENO2 and HSP90B1 expression in HCC cells. Additionally, when ENO2 or HSP90B1 was inhibited, the level of CRP also decreased. Furthermore, CRP co-precipitated and was co-located with ENO2 and HSP90B1 in HCC cells, indicating that CRP may mediate tumor progression, ER stress, and the activation of tumor-related signaling pathways, including PI3K/Akt, by binding to ENO2 or HSP90B1.

Finally, KRT8 and ANXA2 interacted with CRP and exhibited decreased expression in response to CRP silencing. According to previous studies, high KRT8 expression promotes tumor progression and metastasis by regulating epithelial-mesenchymal-transition and cell-matrix adhesion [47]; several annexin A2-interacting proteins mediate tumor progression via the phosphorylation and translocation of annexin A2 to the cell surface [48]. Considering the functions of these proteins, it is reasonable to predict that CRP is involved in the molecular pathogenesis of HCC by interacting with these proteins.

Conclusion

In this study, the CRP-interacting protein network was characterized by Co-IP and iTRAQ based proteomic profiling. The CRP-interacting protein network may activate HCC-related signaling pathways to contribute to the pathogenesis of HCC. The results of this study should be verified in future research.

Acknowledgements

This study was supported by a grant from the National High Technology Research and Development Program of China (863 Program) (No. 2014AA022209), the Natural Science Foundation Project of CQ CSTC (Grant Number: 2012jjA10064), the Natural Science Foundation Project of CQ CSTC (Grant Number: 2013jcyj A 10060), the class General Financial

Grant from the China Postdoctoral Science Foundation (Grant Number: 2012M511912), the Chongqing Postgraduate Research Innovation Project (Grant Number: CYB16095), and the National Science and Technology Major Project of China 2012ZX1002007001, 2011ZX09302005, 2012ZX09303001-001, 2012ZX10002003, 2017ZX10202203-007, and 2017ZX10202203-008).

Disclosure Statement

There are no ethical/legal conflicts related to the article.

References

1 Jemal A, Bray F, Center MM, Ferlay J, Ward E, Forman D: Global cancer statistics. CA Cancer J Clin 2011;61:69-90.
2 Li J, Wang X, Tang J, Jiang R, Zhang W, Ji J, Sun B: HULC and Linc00152 Act as Novel Biomarkers in Predicting Diagnosis of Hepatocellular Carcinoma. Cell Physiol Biochem 2015;37:687-696.
3 Tian H, Huang P, Zhao Z, Tang W, Xia J: HIF-1alpha plays a role in the chemotactic migration of hepatocarcinoma cells through the modulation of CXCL6 expression. Cell Physiol Biochem 2014;34:1536-1546.
4 Beasley RP, Hwang LY, Lin CC, Chien CS: Hepatocellular carcinoma and hepatitis B virus. A prospective study of 22 707 men in Taiwan. Lancet 1981;2:1129-1133.
5 Chen CJ, Yang HI, Su J, Jen CL, You SL, Lu SN, Huang GT, Iloeje UH, Group R-HS: Risk of hepatocellular carcinoma across a biological gradient of serum hepatitis B virus DNA level. JAMA 2006;295:65-73.
6 Liu Y, Wang X, Li S, Hu H, Zhang D, Hu P, Yang Y, Ren H: The role of von Willebrand factor as a biomarker of tumor development in hepatitis B virus-associated human hepatocellular carcinoma: a quantitative proteomic based study. J Proteomics 2014;106:99-112.
7 Karagozian R, Derdak Z, Baffy G: Obesity-associated mechanisms of hepatocarcinogenesis. Metabolism 2014;63:607-617.
8 Dhanasekaran R, Bandoh S, Roberts LR: Molecular pathogenesis of hepatocellular carcinoma and impact of therapeutic advances. F1000Res 2016;5:
9 Gygi SP, Rist B, Gerber SA, Turecek F, Gelb MH, Aebersold R: Quantitative analysis of complex protein mixtures using isotope-coded affinity tags. Nat Biotechnol 1999;17:994-999.
10 Ross PL, Huang YN, Marchese JN, Williamson B, Parker K, Hattan S, Khainovski N, Pillai S, Dey S, Daniels S, Purkayastha S, Juhasz P, Martin S, Bartlet-Jones M, He F, Jacobson A, Pappin DJ: Multiplexed protein quantitation in Saccharomyces cerevisiae using amine-reactive isobaric tagging reagents. Mol Cell Proteomics 2004;3:1154-1169.
11 Deng W, Yan M, Yu T, Ge H, Lin H, Li J, Liu Y, Geng Q, Zhu M, Liu L, He X, Yao M: Quantitative proteomic analysis of the metastasis-inhibitory mechanism of miR-193a-3p in non-small cell lung cancer. Cell Physiol Biochem 2015;35:1677-1688.
12 Ong SE, Blagoev B, Kratchmarova I, Kristensen DB, Steen H, Pandey A, Mann M: Stable isotope labeling by amino acids in cell culture, SILAC, as a simple and accurate approach to expression proteomics. Mol Cell Proteomics 2002;1:376-386.
13 Zhang Y, Hong Q, Huang Z, Xue P, Lv Y, Fu B, Chen X, Wu D: ALDR enhanced endothelial injury in hyperuricemia screened using SILAC. Cell Physiol Biochem 2014;33:479-490.
14 Bantscheff M, Schirle M, Sweetman G, Rick J, Kuster B: Quantitative mass spectrometry in proteomics: a critical review. Anal Bioanal Chem 2007;389:1017-1031.
15 Lin L, Li H, Lin H, Zhang M, Qu C, Yan L, Yin X, Ni J: Application of iTRAQ-Based Quantitative Proteomics Approach to Identify Deregulated Proteins Associated with Liver Toxicity Induced by Polygonum Multiflorum in Rats. Cell Physiol Biochem 2017;43:2102-2116.
16 Ai J, Lu Y, Wei Q, Li H: Comparative Proteomics Uncovers Correlated Signaling Network and Potential Biomarkers for Progression of Prostate Cancer. Cell Physiol Biochem 2017;41:1-9.

17 Yang J, Wezeman M, Zhang X, Lin P, Wang M, Qian J, Wan B, Kwak LW, Yu L, Yi Q: Human C-reactive protein binds activating Fcgamma receptors and protects myeloma tumor cells from apoptosis. Cancer Cell 2007;12:252-265.
18 Volanakis JE: Human C-reactive protein: expression, structure, and function. Mol Immunol 2001;38:189-197.
19 Nozoe T, Saeki H, Sugimachi K: Significance of preoperative elevation of serum C-reactive protein as an indicator of prognosis in esophageal carcinoma. Am J Surg 2001;182:197-201.
20 She S, Xiang Y, Yang M, Ding X, Liu X, Ma L, Liu Q, Liu B, Lu Z, Li S, Liu Y, Ran X, Xu X, Hu H, Hu P, Zhang D, Ren H, Yang Y: C-reactive protein is a biomarker of AFP-negative HBV-related hepatocellular carcinoma. Int J Oncol 2015;47:543-554.
21 Free RB, Hazelwood LA, Sibley DR: Identifying novel protein-protein interactions using co-immunoprecipitation and mass spectroscopy. Curr Protoc Neurosci 2009;Chapter 5:Unit 5 28.
22 Huang BX, Kim HY: Effective identification of Akt interacting proteins by two-step chemical crosslinking, co-immunoprecipitation and mass spectrometry. PLoS One 2013;8:e61430.
23 Yang Y, Lim SK, Choong LY, Lee H, Chen Y, Chong PK, Ashktorab H, Wang TT, Salto-Tellez M, Yeoh KG, Lim YP: Cathepsin S mediates gastric cancer cell migration and invasion via a putative network of metastasis-associated proteins. J Proteome Res 2010;9:4767-4778.
24 Tong SW, Yang YX, Hu HD, An X, Ye F, Hu P, Ren H, Li SL, Zhang DZ: Proteomic investigation of 5-fluorouracil resistance in a human hepatocellular carcinoma cell line. J Cell Biochem 2012;113:1671-1680.
25 Yang Y, Toy W, Choong LY, Hou P, Ashktorab H, Smoot DT, Yeoh KG, Lim YP: Discovery of SLC3A2 cell membrane protein as a potential gastric cancer biomarker: implications in molecular imaging. J Proteome Res 2012;11:5736-5747.
26 Depraetere S, Willems J, Joniau M: Stimulation of CRP secretion in HepG2 cells: cooperative effect of dexamethasone and interleukin 6 Agents Actions 1991;34:369-375.
27 Haider DG, Leuchten N, Schaller G, Gouya G, Kolodjaschna J, Schmetterer L, Kapiotis S, Wolzt M: C-reactive protein is expressed and secreted by peripheral blood mononuclear cells. Clin Exp Immunol 2006;146:533-539.
28 Venugopal SK, Devaraj S, Jialal I: Macrophage conditioned medium induces the expression of C-reactive protein in human aortic endothelial cells: potential for paracrine/autocrine effects. Am J Pathol 2005;166:1265-1271.
29 Kim ES, Cha Y, Ham M, Jung J, Kim SG, Hwang S, Kleemann R, Moon A: Inflammatory lipid sphingosine-1-phosphate upregulates C-reactive protein via C/EBPbeta and potentiates breast cancer progression. Oncogene 2014;33:3583-3593.
30 Pepys MB: C-reactive protein: the role of an ancient protein in modern rheumatology. Clin Exp Rheumatol 1983;1:3-7.
31 Bataille R, Boccadoro M, Klein B, Durie B, Pileri A: C-reactive protein and beta-2 microglobulin produce a simple and powerful myeloma staging system. Blood 1992;80:733-737.
32 Tienhaara A, Pulkki K, Mattila K, Irjala K, Pelliniemi TT: Serum immunoreactive interleukin-6 and C-reactive protein levels in patients with multiple myeloma at diagnosis. Br J Haematol 1994;86:391-393.
33 Legouffe E, Rodriguez C, Picot MC, Richard B, Klein B, Rossi JF, Commes T: C-reactive protein serum level is a valuable and simple prognostic marker in non Hodgkin's lymphoma. Leuk Lymphoma 1998;31:351-357.
34 Pedersen LM, Bergmann OJ: Urinary albumin excretion and its relationship to C-reactive protein and proinflammatory cytokines in patients with cancer and febrile neutropenia. Scand J Infect Dis 2003;35:491-494.
35 Reichle A, Bross K, Vogt T, Bataille F, Wild P, Berand A, Krause SW, Andreesen R: Pioglitazone and rofecoxib combined with angiostatically scheduled trofosfamide in the treatment of far-advanced melanoma and soft tissue sarcoma. Cancer 2004;101:2247-2256.
36 Zhao J, Liu J, Pang X, Wang S, Wu D, Zhang X, Feng L: Angiotensin II induces C-reactive protein expression via AT1-ROS-MAPK-NF-kappaB signal pathway in hepatocytes. Cell Physiol Biochem 2013;32:569-580.
37 Stein MP, Edberg JC, Kimberly RP, Mangan EK, Bharadwaj D, Mold C, Du Clos TW: C-reactive protein binding to FcgammaRIIa on human monocytes and neutrophils is allele-specific. J Clin Invest 2000;105:369-376.
38 Crumley AB, McMillan DC, McKernan M, Going JJ, Shearer CJ, Stuart RC: An elevated C-reactive protein concentration, prior to surgery, predicts poor cancer-specific survival in patients undergoing resection for gastro-oesophageal cancer. Br J Cancer 2006;94:1568-1571.

39 Pine SR, Mechanic LE, Enewold L, Chaturvedi AK, Katki HA, Zheng YL, Bowman ED, Engels EA, Caporaso NE, Harris CC: Increased levels of circulating interleukin 6, interleukin 8, C-reactive protein, and risk of lung cancer. J Natl Cancer Inst 2011;103:1112-1122.

40 Fresno Vara JA, Casado E, de Castro J, Cejas P, Belda-Iniesta C, Gonzalez-Baron M: PI3K/Akt signalling pathway and cancer. Cancer Treat Rev 2004;30:193-204.

41 von Karstedt S, Montinaro A, Walczak H: Exploring the TRAILs less travelled: TRAIL in cancer biology and therapy. Nat Rev Cancer 2017;17:352-366.

42 Buchanan PC, Boylan KLM, Walcheck B, Heinze R, Geller MA, Argenta PA, Skubitz APN: Ectodomain shedding of the cell adhesion molecule Nectin-4 in ovarian cancer is mediated by ADAM10 and ADAM17 J Biol Chem 2017;292:6339-6351.

43 Bouquerel P, Gstalder C, Muller D, Laurent J, Brizuela L, Sabbadini RA, Malavaud B, Pyronnet S, Martineau Y, Ader I, Cuvillier O: Essential role for SphK1/S1P signaling to regulate hypoxia-inducible factor 2alpha expression and activity in cancer. Oncogenesis 2016;5:e209.

44 Alexia C, Fallot G, Lasfer M, Schweizer-Groyer G, Groyer A: An evaluation of the role of insulin-like growth factors (IGF) and of type-I IGF receptor signalling in hepatocarcinogenesis and in the resistance of hepatocarcinoma cells against drug-induced apoptosis. Biochem Pharmacol 2004;68:1003-1015.

45 Vizin T, Kos J: Gamma-enolase: a well-known tumour marker, with a less-known role in cancer. Radiol Oncol 2015;49:217-226.

46 Rachidi S, Sun S, Wu BX, Jones E, Drake RR, Ogretmen B, Cowart LA, Clarke CJ, Hannun YA, Chiosis G, Liu B, Li Z: Endoplasmic reticulum heat shock protein gp96 maintains liver homeostasis and promotes hepatocellular carcinogenesis. J Hepatol 2015;62:879-888.

47 Fang J, Wang H, Liu Y, Ding F, Ni Y, Shao S: High KRT8 expression promotes tumor progression and metastasis of gastric cancer. Cancer Sci 2017;108:178-186.

48 Staquicini DI, Rangel R, Guzman-Rojas L, Staquicini FI, Dobroff AS, Tarleton CA, Ozbun MA, Kolonin MG, Gelovani JG, Marchio S, Sidman RL, Hajjar KA, Arap W, Pasqualini R: Intracellular targeting of annexin A2 inhibits tumor cell adhesion, migration, and *in vivo* grafting. Sci Rep 2017;7:4243.